GENERATION OF SUPER-RESOLUTION IMAGES FROM BLURRED OBSERVATIONS USING MARKOV RANDOM FIELDS

Deepu Rajan

School of Biomedical Engg.
Indian Institute of Technology - Bombay,
Powai, Mumbai - 400 076. India.

Subhasis Chaudhuri

Department of Electrical Engg.
Indian Institute of Technology - Bombay
Powai, Mumbai - 400 076. India.

ABSTRACT

This paper presents a new technique for generating a high resolution image from a blurred image sequence; this is also referred to as super-resolution restoration of images. The image sequence consists of decimated, blurred and noisy versions of the high resolution image. The high resolution image is modeled as a Markov random field (MRF) and a maximum aposteriori (MAP) estimation technique is used. A simple gradient descent method is used to optimize the functional. Further, line fields are introduced in the cost function and optimization using Graduated Non-Convexity (GNC) is shown to yield improved results. Lastly, we present results of optimization using Simulated Annealing (SA).

1. INTRODUCTION

The physical characteristics of a sensor, e.g. its size and density of detectors that form the sensor, limit the resolution of an image. In addition, the bandwidth limit set by the sampling rate also indirectly determines the resolution. These restrictions imposed by the sensor can be overcome by a method known as the super-resolution restoration of images. The underlying philosophy of this method is to acquire more samples of the scene so as to get some additional information which can be utilized, while merging the samples to get a high resolution image. These samples can be acquired by sub-pixel shifts, by changing scene illumination or, as we propose in this paper, by changing the amount of blur. Super-resolved image generation provides a feasible option to sensor modification, which is often not an available option.

Tsai and Huang [1] were the first to propose a frequency domain approach to reconstruction of a high resolution image from a sequence of undersampled low resolution, noise-free images. An iterative backpropagation method is used in [2], wherein a guess of the high resolution output image is updated according to the error between the observed and the low resolution images obtained by simulating the imaging process. A MAP estimator with Huber-MRF prior is described by Schultz and Stevenson in [3]. Elad and Feuer [4] propose a unified methodology for super-resolution restoration from several geometrically warped, blurred, noisy and downsampled measured images by combining ML, MAP and POCS approaches. Chiang and Boult [5] use edge models and a local blur estimate to develop an edge-based super-resolution algorithm.

In this paper, we present a new technique wherein an ensemble of decimated, blurred and noisy observations of an ideal high resolution image are used to generate a super-resolved image. The super-resolved image is modeled as an MRF and a MAP estimation technique is used. Since there is no relative displacement between the input images, the need for estimating sub-pixel shifts does not arise. Also, the input images need not be focused as the algorithm carries out simultaneous restoration (deblurring) in the course of generating the super-resolution image. The proposed method is fast as a result of using a simple gradient-descent minimization of a convex functional. For a non-convex functional that includes line fields, the graduated non convexity algorithm is used for minimization. annealing is required.

In the next section we describe how low resolution images are generated from a high resolution image. In section 3, we cast the super-resolution problem in a restoration framework. The cost function obtained through the MAP estimate is derived in Section 4. Section 5 presents experimental results and conclusions are given in Section 6.

2. LOW RESOLUTION IMAGE FORMATION

We briefly present the formation of a low resolution image from a high resolution image. Note that the problem we solve here is actually the inverse. Suppose the low resolution image sensor plane is divided into $M_1 \times M_2$ square sensor elements and $\{y_{i,j}\}$, $i = 0, \ldots, M_1 - 1$ and $j = 0, \ldots, M_2 - 1$ are the low resolution intensity values. For a decimation ratio of q, the high resolution grid will be of size $qM_1 \times qM_2$ and $\{z_{k,l}\}$, $k = 0, \ldots, qM_1 - 1$ and $l = 0, \ldots, qM_2 - 1$ will be the high resolution intensity values. The forward process of obtaining $\{y_{i,j}\}$ from $\{z_{k,l}\}$ is

written as [3] $y_{i,j} = \frac{1}{q^2} \sum_{k=qi}^{(q+1)i-1} \sum_{l=qj}^{(q+1)j-1} z_{k,l}$ i.e., the low resolution intensity is the average of the high resolution intensities over a neighborhood of q^2 pixels.

Each of the decimated images is blurred by a different, but known linear space invariant blurring kernel. Although more number of blurred samples of a scene do not provide any additional information in the same sense as sub-pixel shifts of the camera or changing illuminant directions do, it is, nevertheless, possible to achieve super-resolution with these blurred samples, as shown in [4]. However, no parametric model for the image is assumed. Finally, i.i.d. zero mean Gaussian noise is added to the decimated and blurred images. Noise is uncorrelated between different low resolution images.

3. PROBLEM FORMULATION

The super-resolution problem is cast in a restoration framework. There are p observed images $\{Y_i\}_{i=1}^{p}$ each of size $M_1 \times M_2$. These images are decimated, blurred and noisy versions of a single high resolution image $\mathbf{z}$ of size $N_1 \times N_2$, where $N_1 = qM_1$ and $N_2 = qM_2$. If $\underline{\mathbf{y_i}}$ is the $M_1M_2 \times 1$ lexicographically ordered vector containing pixels from the low resolution image Y_i, then a vector $\underline{\mathbf{z}}$ of size $q^2M_1M_2 \times 1$ containing pixels of the high resolution image can be formed by placing each of the $q \times q$ pixel neighborhoods sequentially so a to maintain the relationship between a low resolution pixel and its corresponding high resolution pixel. After incorporating the blur matrix and noise vector, the image formation model is written as

$$\underline{\mathbf{y_i}} = H_i D \underline{\mathbf{z}} + \underline{\mathbf{n_i}}, \quad i = 1, \ldots, p \tag{1}$$

where D is the decimation matrix of size $M_1M_2 \times q^2M_1M_2$, H is the blurring matrix (PSF) of size $M_1M_2 \times M_1M_2$, $\underline{\mathbf{n_i}}$ is the $M_1M_2 \times 1$ noise vector and p is the number of low resolution observations. The decimation matrix D consists of q^2 values of $\frac{1}{q^2}$ in each row and has the form [3]

$$D = \frac{1}{q^2} \begin{bmatrix} 1\,1 \ldots 1 & & & 0 \\ & 1\,1 \ldots 1 & & \\ & & \ddots & \\ 0 & & & 1\,1 \ldots 1 \end{bmatrix} \tag{2}$$

Our problem now reduces to estimating $\underline{\mathbf{z}}$ given $\underline{\mathbf{y_i}}$'s, which is clearly an ill-posed problem.

4. MAP ESTIMATE

The maximum a posteriori (MAP) estimation technique is used to obtain the high resolution image $\underline{\mathbf{z}}$ given the ensemble of low resolution images, i.e.,

$$\underline{\hat{\mathbf{z}}} = \arg\max_{\underline{\mathbf{z}}} P(\underline{\mathbf{z}} | \underline{\mathbf{y}}_1, \underline{\mathbf{y}}_2, \ldots, \underline{\mathbf{y}}_p) \tag{3}$$

From Bayes' rule, this can be written as

$$\underline{\hat{\mathbf{z}}} = \arg\max_{\underline{\mathbf{z}}} \frac{P(\underline{\mathbf{y}}_1, \underline{\mathbf{y}}_2, \ldots, \underline{\mathbf{y}}_p | \underline{\mathbf{z}}) P(\underline{\mathbf{z}})}{P(\underline{\mathbf{y}}_1, \underline{\mathbf{y}}_2, \ldots, \underline{\mathbf{y}}_p)}. \tag{4}$$

Since the denominator is not a function of $\underline{\hat{\mathbf{z}}}$, it can be ignored. Taking the log of posterior probability of the numertor of (4), and since $\underline{\mathbf{n}}_i$'s are independent,

$$\underline{\hat{\mathbf{z}}} = \arg\max_{\underline{\mathbf{z}}} \left[\sum_{i=1}^{p} \log P(\underline{\mathbf{y}}_i | \underline{\mathbf{z}}) + \log P(\underline{\mathbf{z}}) \right]. \tag{5}$$

Since noise is assumed to be i.i.d Gaussian,

$$\begin{aligned} P(\underline{\mathbf{y}}_i | \underline{\mathbf{z}}) &= -\sum_{i=1}^{p} \frac{\| \underline{\mathbf{y}}_i - H_i D \underline{\mathbf{z}} \|^2}{2\sigma_\eta^2} \\ &\quad - \frac{M_1 M_2}{2} \log(2\pi\sigma_\eta^2), \end{aligned}$$

where σ_η is the noise variance.

The high resolution image $\underline{\mathbf{z}}$ is now modeled as a Markov random field and hence the prior $P(\underline{\mathbf{z}})$ has a Gibbs distribution given by

$$P(\underline{\mathbf{z}}) = \frac{1}{Z} \exp\{-\sum_{c \in \mathcal{C}} V_c(\underline{\mathbf{z}})\} \tag{6}$$

where Z is a normalizing constant known as the partition function, $V_c(.)$ is the clique potential and $\mathcal{C}$ is the set of all cliques in the image. Thus the estimate can now be written as

$$\underline{\hat{\mathbf{z}}} = \arg\min_{\underline{\mathbf{z}}} \left[\sum_{i=1}^{p} \frac{\| \underline{\mathbf{y}}_i - H_i D \underline{\mathbf{z}} \|^2}{2\sigma_\eta^2} + \sum_{c \in \mathcal{C}} V_c(\underline{\mathbf{z}}) \right] \tag{7}$$

For the cost function in equation (7) to be convex, it is required that the term $V_c(\underline{\mathbf{z}})\}$ be also convex so that the minimization of the function does not get trapped in a local minima. However, as we show later, incorporation of line fields in the cost function followed by optimization using GNC [6] and SA algorithms does result in improved high resolution estimates. We consider pair-wise cliques on a first order neighborhood and impose a quadratic cost which is a function of finite difference approximations of the first order derivative, i.e.

$$V_c(\underline{\mathbf{z}}) = \frac{1}{\lambda} \sum_{k=1}^{N_1} \sum_{l=1}^{N_2} [(z_{k,l} - z_{k,l-1})^2 + (z_{k,l} - z_{k-1,l})^2] \tag{8}$$

Substituting equation (8) in equation (7), we get the final cost function as

$$\begin{aligned} \underline{\hat{\mathbf{z}}} &= \arg\min_{\underline{\mathbf{z}}} \left[\sum_{i=1}^{p} \frac{\| \underline{\mathbf{y}}_i - H_i D \underline{\mathbf{z}} \|^2}{2\sigma_\eta^2} \right. \\ &\quad + \left. \frac{1}{\lambda} \sum_{k=1}^{N_1} \sum_{l=1}^{N_2} [(z_{k,l} - z_{k,l-1})^2 + (z_{k,l} - z_{k-1,l})^2] \right]. \end{aligned}$$

Thus the cost function is quadratic and a simple minimization technique like gradient descent is used to carry out the optimization. The initial estimate $\underline{\mathbf{z}}^{(0)}$ is chosen as the bilinear interpolation of the available least blurred low resolution image. The estimate at $(n+1)th$ iteration, $\underline{\mathbf{z}}^{(n+1)} = \underline{\mathbf{z}}^{(n)} - \alpha g^{(n)}$, where α is the step size and $g^{(n)}$ is the gradient, is computed iteratively until $\| \underline{\mathbf{z}}^{(n+1)} - \underline{\mathbf{z}}^{(n)} \| <$ Threshold. The initial estimate $\underline{\mathbf{z}}^{(0)}$ is chosen as the bilinear interpolation of the available least blurred, low resolution image. Note tha it is the parameteric representation of the super-resolved image $\underline{\mathbf{z}}$ (in terms of the MRF model) that provides the necessary cue for super-resolution.

On inclusion of line field terms [7] in the cost function to account for discontinuities in the image, the gradient descent technique is liable to get trapped in local minima. To avoid such an eventuality, we resort to GNC algorithm for minimizing the modified cost function described below.

The horizontal line field $l_{i,j}$ connecting site (i,j) to $(i,j-1)$ aids in detecting a horizontal edge, while the vertical line field $v_{i,j}$ connecting site (i,j) to $(i-1,j)$ helps in detecting a vertical edge. Note that we have chosen $l_{i,j}$ and $v_{i,j}$ to be binary variables in this study. The log of the prior distribution in equation (6), neglecting the normalizing term, becomes

$$\begin{aligned}\sum_{c\in\mathcal{C}} V_c(\underline{\mathbf{z}}) &= \sum_{i,j} \mu[(z_{i,j}-z_{i,j-1})^2(1-v_{i,j}) \\ &+ (z_{i,j+1}-z_{i,j})^2(1-v_{i,j+1}) \\ &+ (z_{i,j}-z_{i-1,j})^2(1-l_{i,j}) \\ &+ (z_{i+1,j}-z_{i,j})^2(1-l_{i+1,j})] \\ &+ \gamma[l_{i,j}+l_{i+1,j}+v_{i,j}+v_{i,j+1}] \\ &= V(\underline{\mathbf{z}}) \quad (say). \end{aligned} \tag{9}$$

Given a preset threshold, if the gradient at a particular location is above that threshold, the corresponding line field is activated to indicate the presence of a discontinuity. The term multiplying γ provides a penalty for every discontinuity so created. Putting the above expression into equation (7), we arrive at the modified cost function

$$\hat{\mathbf{z}} = \arg\min_{\underline{\mathbf{z}}} \left[\sum_{i=1}^{p} \frac{\| \underline{\mathbf{y}}_i - H_i D \underline{\mathbf{z}} \|^2}{2\sigma_\eta^2} + V(\underline{\mathbf{z}}) \right], \tag{10}$$

which is solved using either the GNC or the SA algorithms.

5. EXPERIMENTAL RESULTS

Figure 1 shows two of the five low resolution noisy images of Lena and CT obtained by decimating the original image and blurring the decimated images with Gaussian blurs of $\sigma = 0.3, 0.5, 0.7, 0.9$ and 1.1. Although the Gaussian blur has infinite extent, for purpose of computation we chose the kernel size corresponding to an extent of $\pm 3\sigma$. Each low resolution image contains zero mean Gaussian noise with variance 5.0. The super-resolved images of Lena and CT,

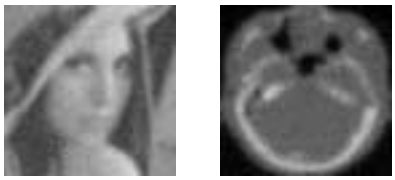

(a) (b)

Fig. 1. One of the low resolution, noisy images of (a) Lena and (b) CT with blur $\sigma = 1.1$.

using all the five low resolution observations are shown in Figures 2 and 3 respectively.

Fig. 2. Super-resolved Lena image using gradient-descent optimization.

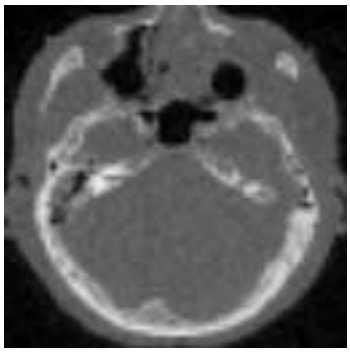

Fig. 3. Super-resolved CT image using gradient-descent.

Next, we present results of minimization of the modified cost function when line processes were used to preserve discontinuity. The GNC algorithm, in which a sequence of convex approximations to the true cost function is optimized, was used for minimization. In our simulations, six approximations to the cost function were minimized using the gradient-descent technique to determine the global minimum. Super-resolved Lena and CT images using the GNC

algorithm are shown in Figures 4 and 5. An improvement in the final estimate of the super-resolved image is seen due

Fig. 4. Super-resolved Lena image using discontinuity preserving method (GNC).

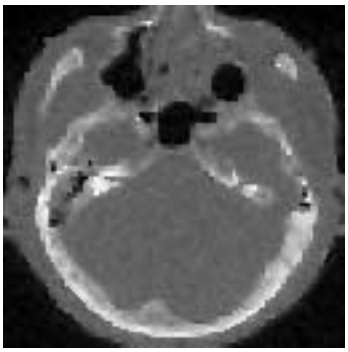

Fig. 5. Super-resolved CT image using discontinuity preserving method (GNC).

to incorporation of line fields in the cost function. Areas in the images with large discontinuities, like the hair portion in the Lena image, have been recovered. Simulations were also carried out to generate the super-resolved image with simulated annealing (SA) using the output of the GNC algorithm as the initial estimate. However, due to paucity of space, we are unable to include the results here. The mean squared error between the original image and generated images is defined as

$$MSE = \frac{\sum_{i=1}^{N_1}\sum_{j=1}^{N_2}(\hat{z}_{i,j} - z_{i,j})^2}{\sum_{i=1}^{N_1}\sum_{j=1}^{N_2}(z_{i,j})^2}. \qquad (11)$$

Table 1 shows the comparison of MSE for the proposed method with standard methods like zero-order hold (ZOH). We include the errors for the case of minimization using simulated annealing (SA) also.

6. CONCLUSIONS

This paper addresses the problem of generating a super-resolution image from a sequence of blurred, decimated and noisy observations of an ideal image. A MAP-MRF approach was used to minimize the function. Comparison with zero order hold shows that the proposed method is superior. Since there is no relative motion between the observed images, as is the case in most of the previous work in super-resolution, the difficult tasks of image registration and motion estimation are done away with. The proposed technique is fast due to optimization using the gradient descent approach. Next, the cost function was modified to include line fields to preserve discontinuitites. In addition to significant noise reduction, the sharpness in the image was also observed to be enhanced.

Method	Lena	CT
ZOH	0.012061	0.899187
Gradient Descent	0.010355	0.021216
GNC	0.009473	0.021085
SA	0.008820	0.007615

Table 1. Comparison of MSEs of different interpolation schemes.

7. REFERENCES

[1] R. Y. Tsai and T. S. Huang, "Multiframe image restoration and registration," in *Advances in Computer Vision and Image Processsing*, pp. 317–339, JAI Press Inc., 1984.

[2] M. Irani and S. Peleg, "Improving resolution by image registration," *CVGIP:Graphical Models and Image Processing*, vol. 53, pp. 231–239, March 1991.

[3] R. R. Schultz and R. L. Stevenson, "A Bayesian approach to image expansion for improved definition," *IEEE Trans. on Image Processing*, vol. 3, pp. 233–242, May 1994.

[4] M. Elad and A. Feuer, "Restoration of a single superresolution image from several blurred, noisy and undersampled measured images," *IEEE Trans. on Image Processing*, vol. 6, pp. 1646–1658, December 1997.

[5] M.-C. Chiang and T. E. Boult, "Local blur estimation and super-resolution," in *Proc. CVPR, Puerto Rico, USA*, pp. 821–826, 1997.

[6] A. Blake and A. Zisserman, *Visual Reconstruction*. MIT Press, 1987.

[7] S. Geman and D. Geman, "Stochastic relaxation, Gibbs distribution and the Bayesian restoration of image," *IEEE Trans. on Pattern Analysis and Machine Intelligence*, vol. 6, no. 6, pp. 721–741, 1984.